

---

# WEAR AT ELEVATED TEMPERATURES - MICROSTRUCTURAL INVESTIGATIONS OF TOOL MATERIALS AFTER HIGH TEMPERATURE SLIDING WEAR

M. Walter<sup>1</sup> ([walter@wtech.rub.de](mailto:walter@wtech.rub.de), phone: +49(0)234-32-25962, fax: + 49(0)234-32-14104),

G. Egels<sup>1</sup>, A. Röttger<sup>1</sup>, W. Theisen<sup>1</sup>

<sup>1</sup>Lehrstuhl Werkstofftechnik, Ruhr-Universität Bochum, 44801 Bochum, Germany

## Abstract

The presented study investigates the hardness and sliding wear behavior of cemented carbides and high-speed tool steels at elevated temperatures. Therefore, experimental analysis focus on the behavior and the microstructural changes of the aforementioned materials during sliding wear at room temperature, 400°C, and 600°C. Investigations are performed with respect to materials mechanical properties, which are represented by high temperature hardness measurements. As a result a main output of this study is an overview about the interdependencies of the microstructure and the high temperature hardness of tool materials (cemented carbides, high-speed steels). Results show that the absolute value of the room temperature and the high temperature hardness of cemented carbides are connected to the WC-carbide volume fraction. In contrast, the development of the hardness with increasing temperature is mainly influenced by the volume fraction and the characteristics of the binder matrix. In addition to the investigation of cemented carbides, the hardness of HS 6-5-3 steel grade at elevated temperatures was investigated. The value of the high temperature hardness of HS 6-5-3 high-speed steel is comparable to the hardness of cemented carbide materials, having higher binder content of 30 vol.-%. The absolute value and the temperature dependent course of the high temperature hardness of the high-speed steel are further influenced by the applied heat-treatment. Moreover, detailed wear experiments and microscopic analyses of the worn surfaces of selected materials are presented. These investigations show the main differences between room temperature sliding wear and high temperature sliding wear. In the systems studied, an increase in testing temperature leads to a rapid decrease of friction and wear rate. Microscopic investigations reveal that, the reason for this effect is the formation of a tribochemical wear layer at the surface of the wear bodies. This layer suppresses direct metallic contact and changes the characteristics of the tribological system. Discussed issues of high temperature sliding wear are the formation and stability of tribochemical wear layers, their connection to and support by the bulk material as well as the fracturing and damage of the layer-bulk-material compound.

**Keywords:** High temperature sliding wear, high temperature hardness, cemented carbides, high-speed steel, tribochemical wear layer

## Introduction

Hot rolling is a key process of the industrial manufacturing chain of steel products. This forming process utilizes the low yield strength and increased formability of steels at elevated temperatures to enable lower rolling forces and higher degrees of reduction at the same time. Nevertheless, the contact of the roll surface and the hot product leads to a high temperature stress of the roll material. Roll materials have to endure the combination of high rolling forces and thermal stresses at the same time [1]. The relative motion between the roll surface and the product further promotes high temperature sliding wear. Therefore, materials used for hot rolling need to combine high strength and wear resistance at elevated temperatures [2]. Mechanical features like high temperature hardness consequently decide if and at which point of the hot rolling production line a

material can be used. Conventionally used materials of the intermediate and finishing stands of hot rolling lines are cemented carbides and high-speed steels. These materials combine a high hardness and a high wear resistance at elevated temperatures [1]. Nevertheless, the microstructural behavior of these materials under high temperature sliding wear has been investigated and compared insufficiently. Therefore, this study focuses on the sliding wear behavior of cemented carbide and high-speed steel materials at elevated temperatures with respect to mechanical properties, microstructural changes and the formation of tribochemical wear layers.

## 1. Experimental

### Materials and heat treatment

The chemical compositions of the investigated materials and their hardness at room temperature are given in **Table 1**.

**Table 1:** Chemical composition (mass-%) and properties of the investigated materials in initial state

Notation	Co	Ni	Cr	W	V	Si	C	Fe	Hardness in HV10
WC- 10 mass-% Co	10.0	-	-	-	-	-	-	-	1736
WC- 30 mass-% Co	30.0	-	-	-	-	-	-	-	632
WC- 30.5 mass-% Co, Ni, Cr	14.0	15.0	1.5	-	-	-	-	-	589
C60	-	0.4	0.4	-	-	0.4	0.57	Bal.	216
HS 6-5-3 (QT)	-	-	4.0	6.4	2.8	0.5	0.90	Bal.	643

For experiments squared specimens (10 x 10 x 4 mm) of the cemented carbides, the high-speed steel (HSS) and the C60 steel were prepared. Steel grade C60 was further used as the counterbody in the wear experiments. Therefore, hemispheres ( $r = 5$  mm,  $h = 10$  mm) were produced from this material and heat-treated in accordance to the industrial manufacturing route (austenitized at 1000°C followed by a slow furnace cooling within 2h down to room temperature) to achieve a ferritic-pearlitic microstructure.

Cemented carbides were used in initial state, produced by liquid phase sintering. In contrast, HS 6-5-3 high-speed steel was used in as-cast quality and in heat-treated condition, further indicated as QT. The steel HS 6-5-3 was soft annealed at 650°C/ 6 h, air-quenched from 1150°C/ 15 min. and tempered three times at 500 – 620°C/ 2 h. [3]. After the heat-treatment, the surface of the specimens was ground with 18  $\mu$ m abrasive paper and polished with a 3  $\mu$ m and 1  $\mu$ m diamond paste and  $\frac{1}{4}$   $\mu$ m SiO<sub>2</sub> polishing suspension. Experiments were done in this microstructural surface condition to enable comparable experimental conditions.

Microstructural examinations were performed by means of scanning electron microscopy (SEM) using a MIRA3 TESCAN SEM. Figures were taken at a working distance of 15 mm and an acceleration voltage of 20 keV in secondary electron (SE1) mode.

### Hardness measurements and wear experiments

Wear and hardness experiments were performed with an Optimol SRV4 measuring device. Hardness testing was done by a specific modification of the measuring device. The measurements were carried out in accordance to DIN EN ISO 6507-1 with an applied load of 98.07 N (HV10) in a temperature range from room temperature (25°C) to 800°C. To avoid a strong oxidation of the surface of the specimen during testing, forming gas was used. High temperature hardness measurements were done using all aforementioned materials in heat-treated conditions. High temperature wear experiments were only done using the combinations C60 steel (pin) versus WC-30.5 mass-% Co, Ni, Cr (disc) and C60 steel (pin) versus HS 6-5-3 (disc). During the wear experiments polished C60 pins were tested against the polished surface of WC- 30.5 mass-% Co, Ni, Cr and HS 6-5-3 discs with a frequency of 30 Hz over a stroke distance of 1.5 mm applying a

normal force of 30 N ( $t = 1.5$  h) in a sliding wear test. In accordance to the actual industrial process wear experiments were performed in air. Measured quantities of the sliding wear experiments are the volume loss of the C60 steel pin, the time dependent friction coefficient and the time dependent integral wear path of the tribological system.

The integral wear path is a measured quantity which contains information about the total wear occurring in the regarded system. It displays the height-loss of the pin and the disc sample in combination. Therefore, this value is a parameter of the entire system and not of a single constituent. Due to the measurement of the height of the pin and disc combination, thermal expansion during testing at elevated temperatures influences the value of the integral wear path strongly. This thermal influence needs to be regarded to avoid a systematic error. In this study the influence of the thermal expansion on the results of the wear tests was considered by a number of pre-tests. Pre-testing consisted of an exact determination of the temperature at the contact point of pin and disc, as well as several neutral temperature and thermal expansion tests with no motion between the parts. Using these neutral tests it was possible to determine the testing temperatures of pin and disc very precisely. Further it was possible to determine the critical point of thermal stability of the testing system. After this point thermal expansion reaches a constant level and wear tests can be performed under constant conditions.

## 2. Results and Discussion

In the first section, the results of the high temperature experiments using cemented carbides are presented. On the one hand, the investigations focus on the measured results of the hardness and wear experiments. On the other hand the microstructural changes of the cemented carbide materials during sliding wear at different temperatures are investigated. The second section deals with the corresponding results of the high temperature experiments using HS 6-5-3 steel.

### 2.1 High temperature properties and sliding wear behavior of cemented carbides

The microstructure of cemented carbides consists of a binder matrix (Co, Ni etc.) and a high volume fraction of tungsten carbide as a hard phase. The mechanical properties of cemented carbide materials are determined by the fractions and characteristics of these two components [4]. The materials WC- 10 mass-% Co and WC- 30 mass-% Co are a combination of a Co-matrix and a varying amount (90 or 70 mass-%) of WC-carbides. Besides the different Co-binder weight fractions the used materials possess different WC-carbide grain sizes (**Fig. 1**). While the grain size of WC- 10 mass-% Co is fine ( $< 1 \mu\text{m}$ ) the grain size of WC- 30 mass-% Co is rather coarse (1-5  $\mu\text{m}$ ). These facts lead to a large difference of the room temperatures hardness of the materials [4]. The hardness of sample WC-10 mass-% Co is nearly 1100 HV10 higher than the hardness of sample WC- 30 mass-% Co. The difference of the room temperature hardness of the materials WC- 30 mass-% Co and WC- 30.5 mass-% Co, Ni, Cr (**Fig. 2**) is less pronounced. Although containing different binder compositions these cemented carbides have a similar hardness. In this case the nearly equal size and the amount of WC-carbides lead to comparable properties. The WC-carbide amount has a dominant influence on the mechanical properties, especially on the hardness and the bending strength [5]. An increase of the WC-carbide volume fraction increases the hardness strongly, while a change of the binder composition has only a minor influence.

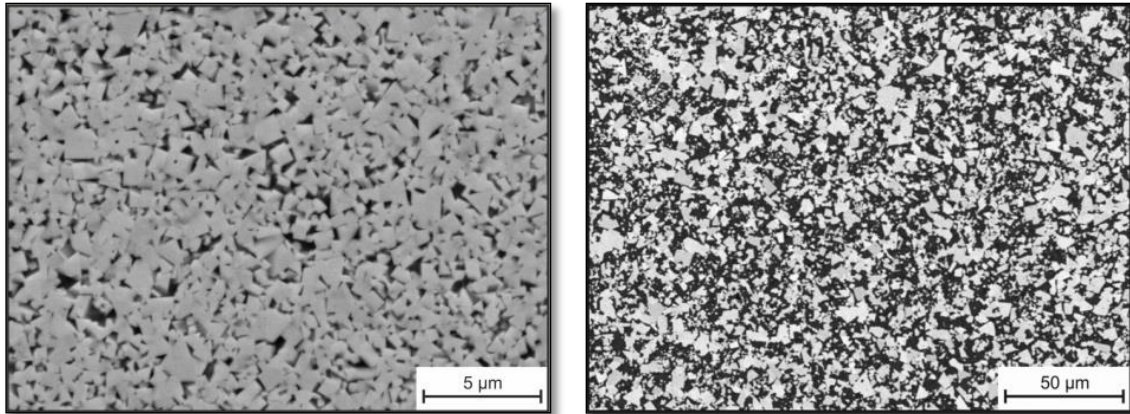


**Fig. 1:** SEM micrographs of the initial microstructure of the cemented carbide WC- 10 mass-% Co (left) and WC- 30 mass-% Co (right)

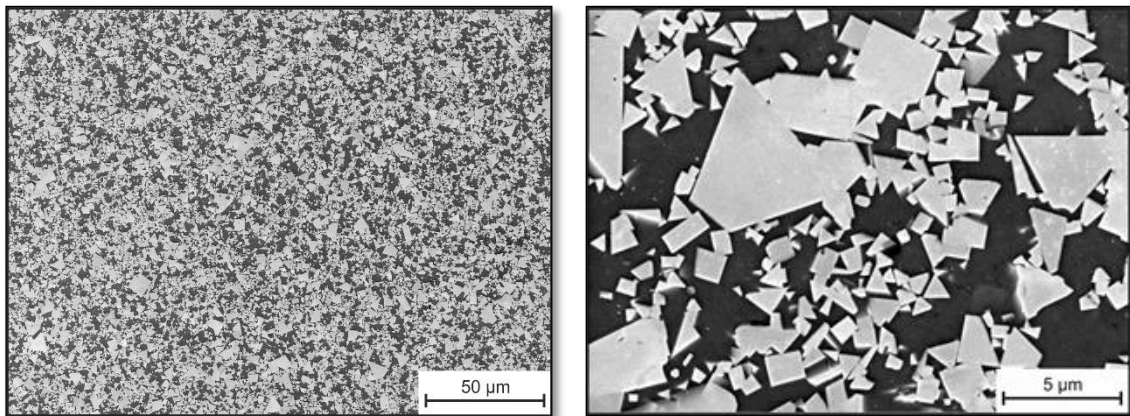


**Fig. 2:** SEM micrographs of the initial microstructure of the cemented carbide WC- 30.5 mass-% Co, Ni, Cr (left), close-up of the WC-carbide distribution (right)

**Fig 3. a)** shows that the room temperature results and correlations of the hardness of cemented carbides can be transferred to elevated temperatures. The depiction of the hardness depending on temperature of the cemented carbides shows the same hardness ratio between the materials at room temperature as well as at high temperature. Furthermore it can be seen that, the hardness of WC- 30 mass-% Co and WC- 30.5 mass-% Co, Ni, Cr decreases constantly with increasing temperature. In opposite the high room temperature hardness of WC- 10 mass-% Co decreases steeply with increasing testing temperatures. Reaching a temperature of 600°C the hardness of WC- 10 mass-% Co is about 25 % lower than the room temperature value. An even more pronounced hardness decrease occurs exceeding a temperature of 600°C. In a temperature range from 600 to 800°C hardness of sample WC-10 mass-% Co decreases to a value of about 600 HV10. These results show that the mechanical properties of WC- 10 mass-% Co are much more sensitive to a temperature increase than the properties of cemented carbide materials which contain a larger binder amount. Cemented carbides with a lower WC-content show much more stable high temperature hardness than WC- 10 mass-% Co. This behavior of WC- 10 mass-% Co can be traced back to its high overall hardness. Due to the much higher absolute value of hardness the hardness degradation at elevated temperatures is more pronounced. An additional explanation focusses on the fact that cemented carbides, which contain large fractions of WC-carbides, behave similar to polycrystalline WC. Cemented carbides with lower binder content are significantly harder than binder rich grades and show equal mechanical properties than single crystal WC-carbide. Furthermore, their hardness decreases very rapidly with increasing temperature, behaving again similar to single crystal WC-carbide [6]. Indentation can take place more easily at elevated temperatures, because of the rapid hardness loss. This lowers the wear resistance of cemented

carbides with high binder fractions at elevated temperatures, because of unstable high temperature properties. Cemented carbides containing a higher binder fraction show more stable properties at elevated temperatures. The higher binder fraction provides a better support of the WC-carbides. The binder phase excellently integrates the hard phases at elevated temperatures, because of more stable mechanical properties. This leads to a better performance of binder rich cemented carbides at elevated temperatures [7]. Consequently, hard phases are able to increase the wear resistance of these materials effectively. Therefore, WC- 30 mass-% Co and WC- 30.5 mass-% Co, Ni, Cr are suitable materials for applications stressed by high temperature sliding wear. According to this conclusion and to the fact that the high temperature hardness and microstructures of WC- 30 mass-% Co and WC- 30.5 mass-% Co, Ni, Cr do not differ significantly, only WC- 30.5 mass-% Co, Ni, Cr was regarded in sliding wear experiments. High temperature wear tests were done with the intention of finding general and specific aspects of the high temperature sliding wear behavior of cemented carbides. Experiments were done using a WC-30.5 mass-% Co, Ni, Cr basic body (disc) and C60 steel as the counter body (pin). Therefore, **Fig. 3 a)** shows the hardness as a function of temperature of C60 steel. The comparison of the hardness of WC- 30.5 mass-% Co, Ni, Cr and C60 steel shows that independent of the testing temperature the hardness of C60 steel is lower than the hardness of WC- 30.5 mass-% Co, Ni, Cr. C60 steel will be the primary worn element of the regarded tribological system. The further analyses of wear mechanisms of the WC- 30.5 mass-% Co, Ni, Cr basic body need to consider this fact. **Fig. 3 b) to d)** present the results of the wear experiments (pin: C60/ disc: WC- 30.5 wt.% Co, Ni, Cr) at 25°C, 400°C and 600°C. The diagram of the volume loss of the C60 steel pin (**Fig.3 b)** shows a strong decrease of the volume loss of the pin by increasing the testing temperature from 25°C to 400°C [8]. The worn volume of C60 steel pin decreases in this temperature range to less than 10 % of the room temperature value. With a further increase of the testing temperature the volume loss of C60 steel pin shows no further decrease and rather shows a slightly growing volume loss. In addition to this **Fig. 3 c)** and **d)** show the time dependent integral wear path and friction coefficient during wear experiments. The course of the integral wear path depending on time is shown in **Fig. 3 c)**. The graph of the experiment performed at 25°C shows a non-linear increase of the integral wear path during the first period of the test. The integral wear path increases strongly during this period. After this period the increase changes and becomes linear. It can be concluded that at the beginning of the presented room temperature sliding wear tests a bedding-in period occurs. After this period the system shows a constant wear behavior. The courses of the integral wear paths of the experiments at elevated temperature differ from the room temperature experiment. Firstly, the courses of the integral wear paths at elevated temperatures don't show a sharp increase at the beginning of the wear experiment. Secondly, the wear-rates at elevated temperatures are approximately independent on time. The increase of the integral wear path is continuous during the entire experiment. Furthermore, some discontinuities occur during the experiment. These discontinuities couldn't be prevented even after several repetitions of the tests. The ratio of the integral wear paths of the test at 400°C and 600°C are in accordance with the results of the measured volume loss of the C60 steel pin. The integral wear paths of the test performed at 600°C as well as the volume loss of the pin exceed the values measured during the test at 400°C. The results from the time dependent measurement of the friction coefficient complete the presented study. The friction coefficients of the wear tests at room temperature and elevated temperatures differ from each other strongly. The high temperature experiments show high friction coefficients, which scatter continuously and largely around a mean value. In addition, the friction coefficients scatter discontinuous with large deflections [8]. The room temperature wear test in opposite shows two periods of the development of the friction coefficient and less scattering. The friction coefficient decreases steadily during the first period of the experiment. After this it reaches a constant value and levels around this value with only minor scattering. The course of the friction coefficient shows no large deflections.



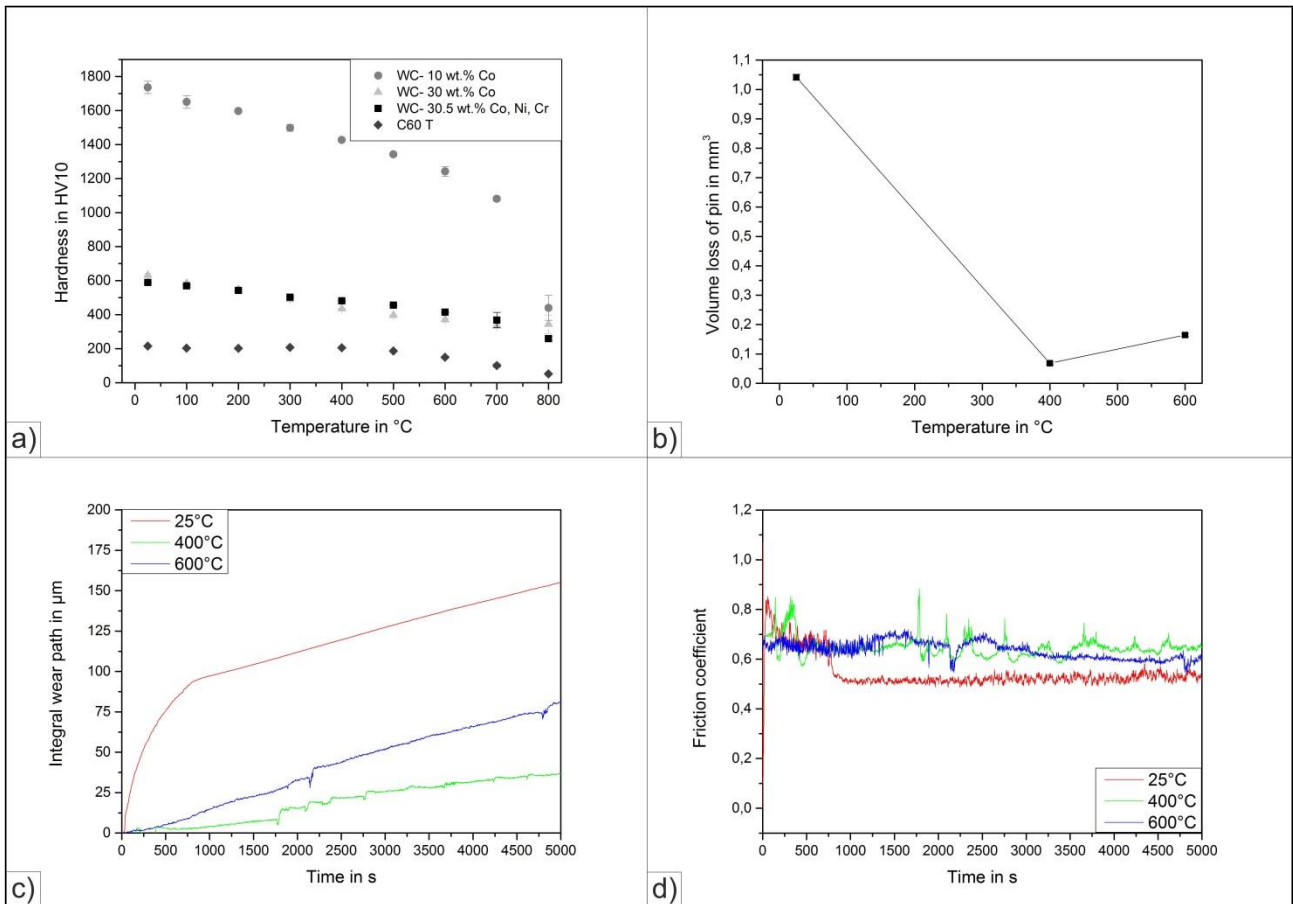


**Fig. 3:** a) Hardness depending on temperature of the cemented carbides and C60 steel, b) Volume loss of C60 steel pin during wear tests at 25°C, 400°C and 600°C, c) Integral wear path depending on time, d) Friction coefficient depending on time during wear tests at 25°C, 400°C and 600°C (pin: C60/ disc: WC- 30.5 mass-% Co, Ni, Cr)

To explain the ratios and developments of the wear rates and friction coefficients at different temperatures, it is necessary to investigate the microstructures of the cemented carbide material after sliding wear. Therefore, **Fig. 4** to **6** show SEM micrographs of the wear scar microstructures of the cemented carbide, tested at different temperatures.

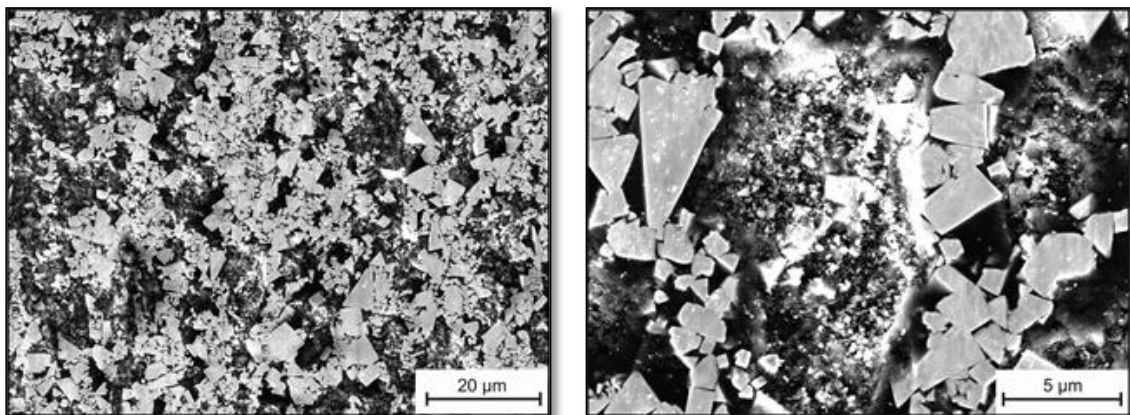


**Fig. 4:** SEM micrographs of the wear scar microstructure of the cemented carbide WC- 30.5 mass-% Co, Ni, Cr after 25°C wear test (pin: C60/ disc: WC- 30.5 mass-% Co, Ni, Cr)

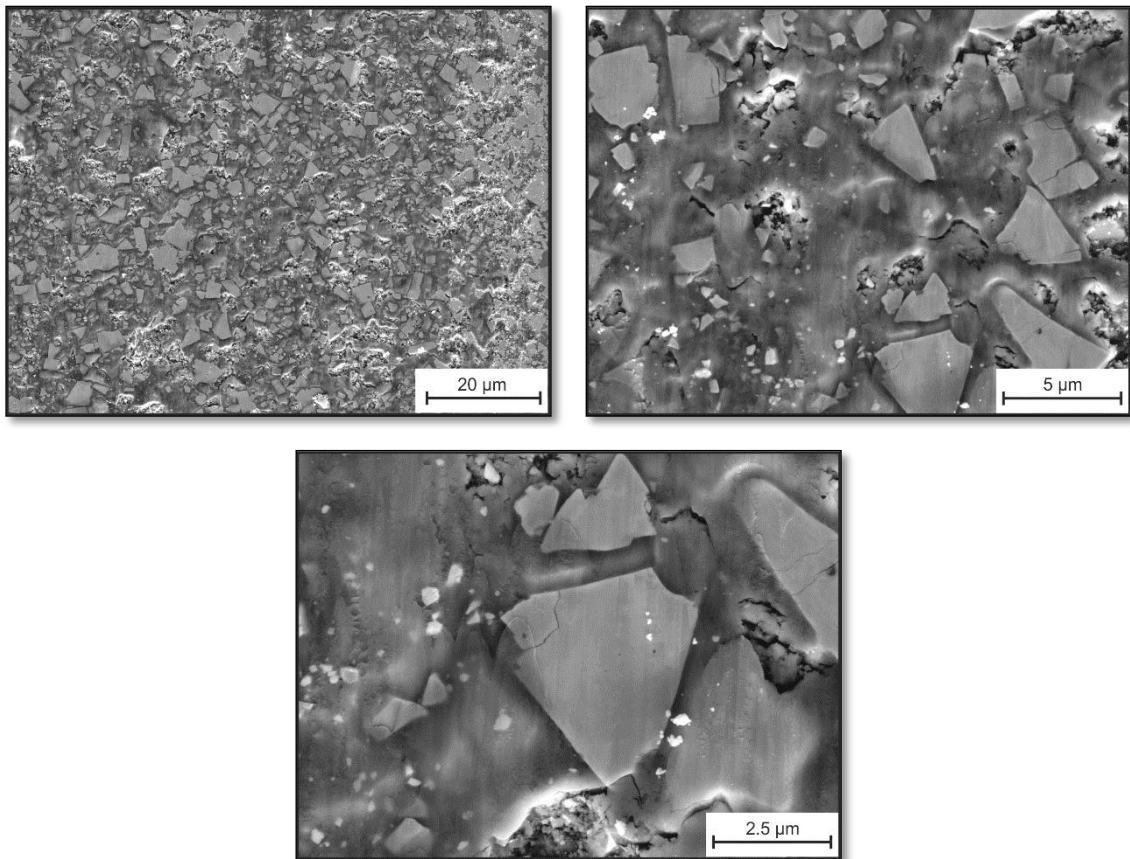


**Fig. 5:** SEM micrographs of the wear scar microstructure of the cemented carbide WC- 30.5 mass-% Co, Ni, Cr after 400°C wear test (pin: C60/ disc: WC- 30.5 mass-% Co, Ni, Cr)

The microstructure of the cemented carbide (**Fig. 4**) after the wear experiment performed at room temperature consists of a dominant amount of exposed WC-carbides. WC-carbides show no large impact of sliding wear. In comparison to the initial state, the shape and the distribution of the WC-carbides in the microstructure of the cemented carbide are unaffected. In contrast, the binder-matrix is affected strongly [9]. The matrix appears rough and cleft. Furthermore, a lot of wear particles are localized in the matrix areas. These observations indicate that the impact of a sliding wear exposure of cemented carbide at room temperature is mainly influenced by the binder-matrix. The tungsten carbides are only minor affected. Furthermore, it can be concluded that, the major amount of wear in the investigated tribological system is located at the much softer C60 steel pin. A comparison of the components of the tribological system shows that, the hardness and the content of hard phases of the cemented carbide are much higher. C60 steel possesses a lower wear resistance in contrast to cemented carbide, resulting in a higher mass loss of the C60 pin during testing. Nevertheless, the binder-matrix of the cemented carbide material shows signs of wear impact as well [9]. Thus, the properties of the binder-matrix are key factors which determine the wear behavior of cemented carbide materials and need to be considered during microstructural investigations in detail. The influence of an increased testing temperature on the wear behavior of cemented carbide materials can be seen in **Fig. 5** and **6**. The microstructures of the worn samples after high temperature testing differ significantly from the microstructures tested at room temperature. The main difference can be found in the formation of a tribochemical wear layer during high temperature wear. During wear the gathering of wear products (oxides, carbides and other wear particles) in the matrix areas leads to the formation of a well densified surface layer consisting of hard phases and wear products. This layer covers the whole wear scar. At 400°C the surface of the wear scar appears dense and well integrated. The WC-carbides are embedded into a compact layer. The matrix between the hard phases is compact and no large gaps between the carbides are visible. Nevertheless, cracks and small fractures occur in the layer.

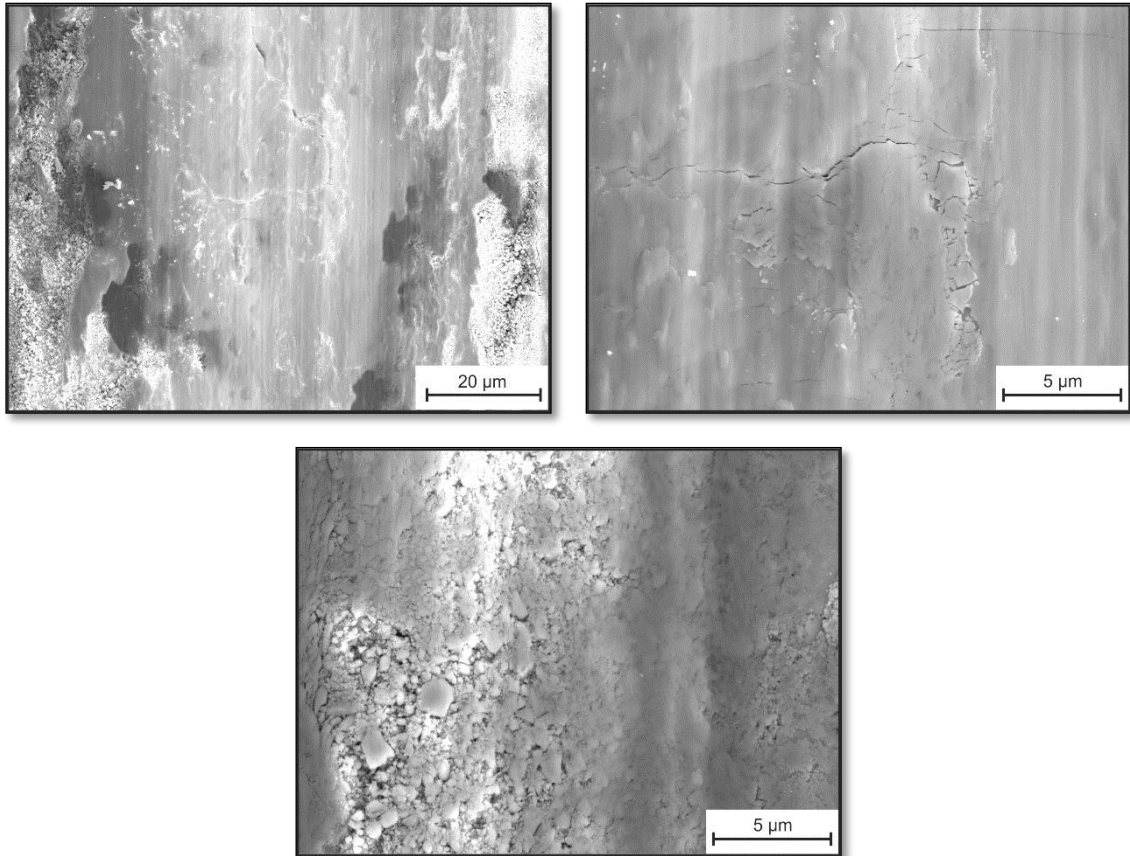


**Fig. 6:** SEM micrographs of the wear scar microstructure of the cemented carbide WC- 30.5 mass-% Co, Ni, Cr after 600°C wear test (pin: C60/ disc: WC- 30.5 mass-% Co, Ni, Cr)

Furthermore, the WC-carbides which are embedded into this layer show damages. Cracks occur through the hard phases and especially at their sharp edges. This damage of the hard phases did not occur during room temperature testing [10]. Reasons for this damage are assumed to be connected with the formation of the tribochemical wear layer and the embedding of the hard phases into this layer. It can be assumed, that the differences of the Co-base binder matrix and the wear layer properties (tensile strength and deformability) lead to this effect. The support of the hard phases by the binder matrix decreases during high temperature sliding wear. Thermal softening and the lower strength of the wear layer matrix, thereby promote brittle failure of the WC-carbides. Therefore, the formation of the tribochemical wear layer dominates the wear behavior of the cemented carbides at elevated temperatures. A self-protection of the components of the tribological system occurs, because the wear layer separates the components. This leads to lower wear of the cemented carbide disc and the C60 steel pin, because of no direct contact of the metallic materials. Nonetheless, a tribochemical wear layer formed by compacted particles suffers from low mechanical stability. Cracks and fractures, especially along the matrix-hard-phase-interface, exist in large number. These imperfections of the layer lead to the failure of the self-protection layer at a certain point respectively layer thickness. Damage occurs, parts of the layer and hard phases fracture and wear as well as friction increase. This effect leads to jumps in the curves of the integral wear path and the friction coefficient. Therefore, it can be concluded that the benefit of a self-protection layer is bordered by its stability. A thick and weakly compacted layer will fracture easily under mechanical load, leading to an increase in wear and friction. This effect is assumed to take place during the wear experiments at 600°C. The wear layer grows at this temperatures much more pronounced, leading very quickly to a critical thickness. A mechanical stressing of this instable surface leads to the failure of the tribochemical wear layer (**Fig. 6**).



## 2.2 High temperature properties of and wear behavior of HS 6-5-3 steel

The microstructure of the high-speed tool steel HS 6-5-3 is displayed in **Fig. 7**. In quenched and tempered state this steel possesses a hardness of approx. 640 HV10. The microstructure consists of annealed martensite and carbides of types MC, M<sub>2</sub>C and M<sub>6</sub>C [11, 12].

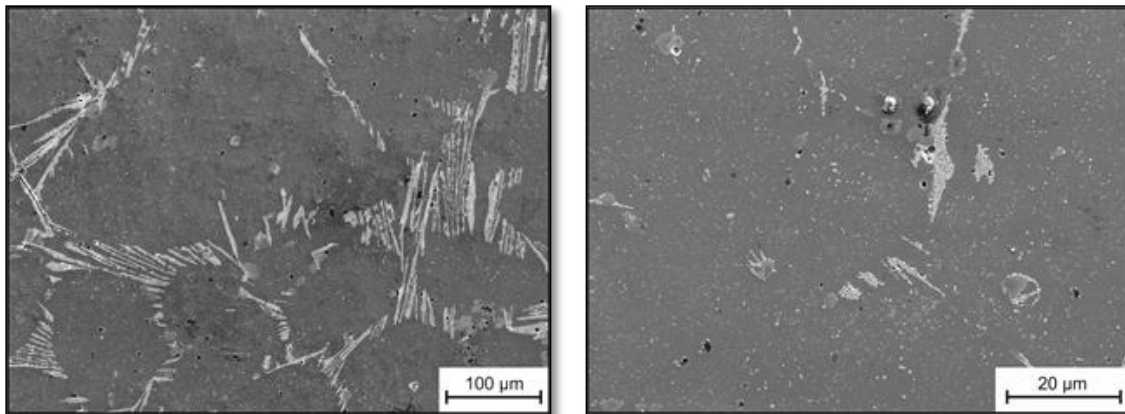


**Fig. 7:** SEM micrographs of the microstructure of the high-speed steel HS 6-5-3 in quenched and tempered state

Similar to the experiments performed in **section 2.1** the HSS was investigated due to its high temperature hardness and its performance during high temperature sliding wear (**Fig. 8**). **Fig. 8 a)** shows the development of the hardness of this steel as a function of temperature. Till 500°C the hardness decreases only slightly and in a constant way. Exceeding a temperature of 500°C the decrease in hardness is more pronounced, as a result a low hardness of less than 250 HV10 can be found at a temperature of 800°C. The strong decline in hardness falls exactly beyond the temperature range of the maximum tempering temperatures (500–600°C). Above this temperature the well-defined and stabilized microstructure during heat-treatment is affected by thermal softening mechanisms again pronouncedly. This results in a strong decrease in hardness. Therefore, the use of high-speed tool steels at elevated temperatures is affected and limited by the applied heat-treatment strongly [11]. The tempering stabilizes the mechanical properties of a HSS till a certain temperature. Above this temperature microstructural changes reoccur, leading to an unpredictable behavior of the material and the structural component. Regarding this fact the maximum tempering temperature of the studied HSS needs to be chosen above the maximum testing temperature. The performance of the HSS during sliding wear tests is shown in **Fig. 8 b)** to **d)**. Similar to the results of the wear experiments using the cemented carbide basic body, the wear rates (**Fig. b** and **c**) of these tests decrease with increasing temperature. Furthermore, the wear rates at any temperatures are lower than in the experiments presented in **section 2.1**. In contrast, the development of the time dependent friction coefficients depending on temperature differs from the previous presented courses. The courses of the friction coefficient between HSS and C60 steel during sliding wear show a contrarily development. At room temperature the friction coefficient is very high and is characterized by a large scattering [13]. At elevated temperatures the friction coefficient decreases and scatters only little.

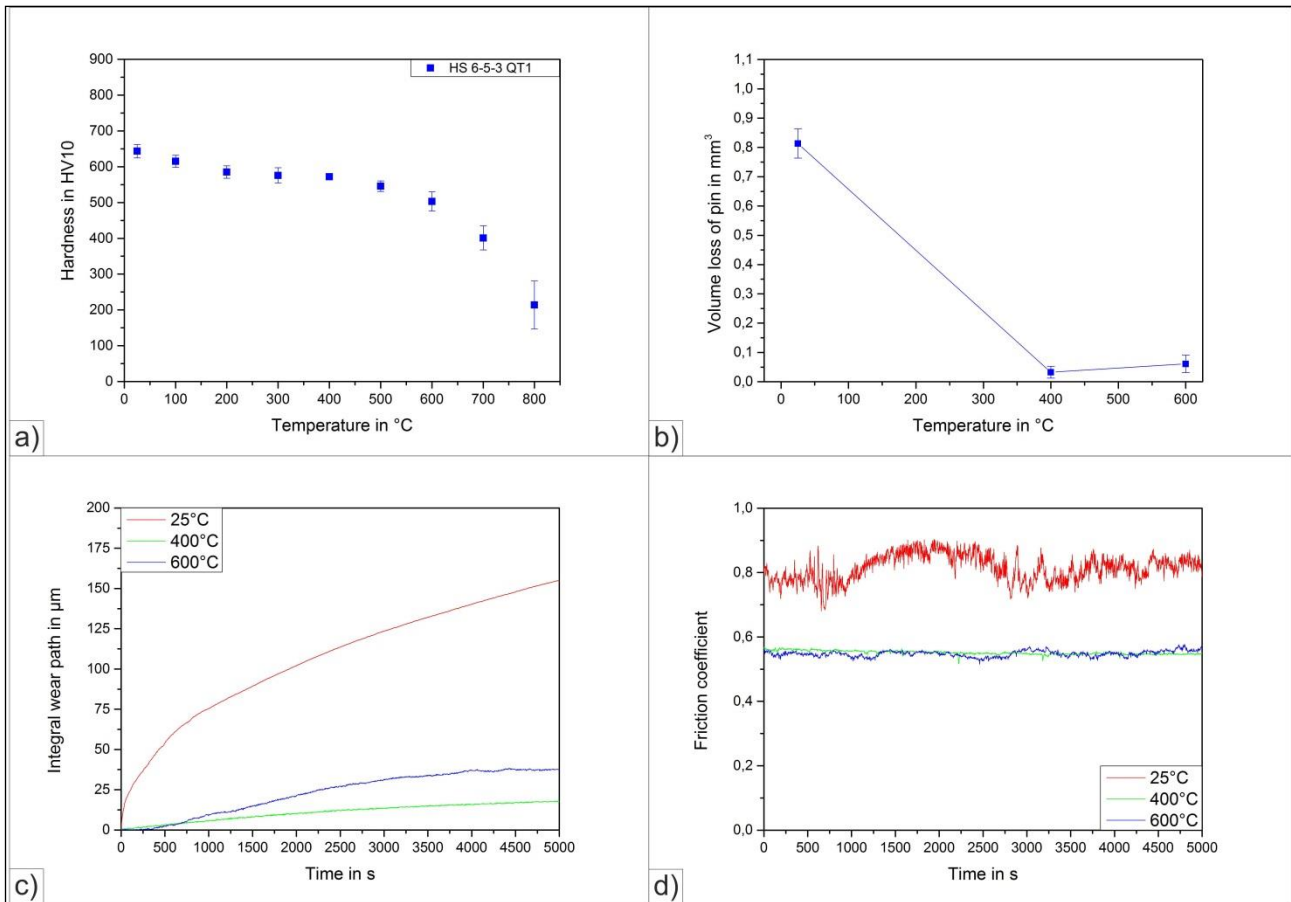


**Fig. 8:** a) Hardness depending on temperature of the steel HS 6-5-3 in quenched and tempered condition, b) Volume loss of C60 steel pin during wear tests at 25°C, 400°C and 600°C, c) Integral wear path depending on time, d) Friction coefficient depending on time during wear tests at 25°C, 400°C and 600°C (pin: C60/ disc: HS 6-5-3 in quenched and tempered condition)

With respect to the aforementioned results **Figs. 9 to 11** show the corresponding wear scars of the HSS basic bodies after sliding wear tests. Similar to the results obtained by the tests of **section 2.1** a change of the wear scar microstructure depending on testing temperature can be observed. The worn surfaces produced by experiments at elevated temperatures are covered by a tribochemical wear layer. The room temperature wear scars in opposite still indicate the initial high-speed steel microstructure after wear testing for 1.5 h (**Fig. 9**). More detailed analyses of these wear scars show grooves in the metal-matrix and small, loose wear particles. The carbides in the high-speed steel microstructure are less influenced by wear. Carbides are not scratched or ploughed and are well embedded in the steel matrix. Furthermore, wear products are agglomerated at the different types of carbides [14, 15].

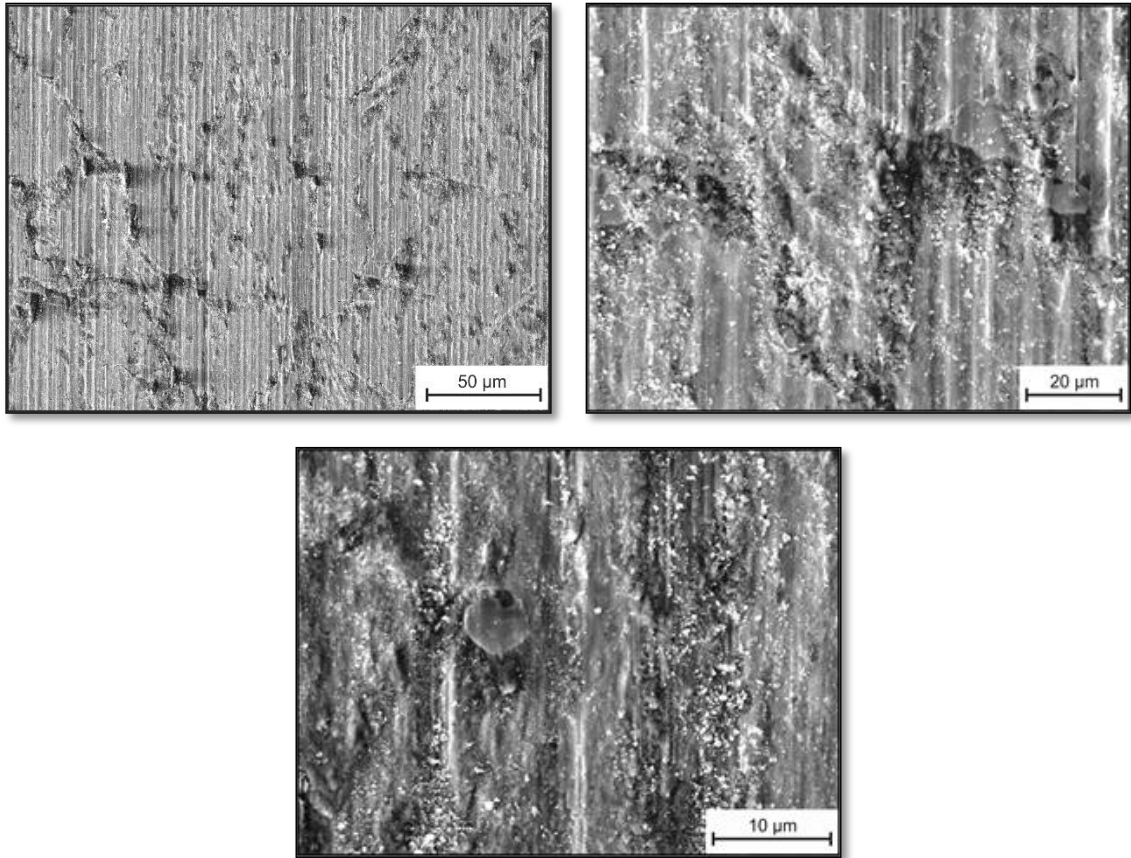


**Fig. 9:** SEM micrographs of the worn microstructure of the steel HS 6-5-3, after 25°C wear test (pin: C60/ disc: HS 6-5-3 QT1)

The wear scars resulting from experiments at elevated temperatures are entirely covered by a tribochemical wear layer. No indications of the initial microstructure can be detected from a top view of the worn samples at a temperature of 400°C. Further the tribochemical wear layer produced by testing at 400°C and 600°C are not similar and indicate different structures. The wear scar resulting from 400°C sliding wear test is covered entirely with a partly dense and partly fractured layer (**Fig. 10**). This tribochemical layer appears mainly oxidic. The SEM analyses show that the layer consist of compacted wear products. These products form an oxide-rich intermediate phase between the high-speed steel and C60 steel, which lowers wear at elevated temperature by preventing direct metallic contact. Unfortunately a lot of areas of this layer show large cracks and fractures. The high brittleness of the oxide layer leads to a quick crack initiation resulting in pronounced failure under mechanical load [16].

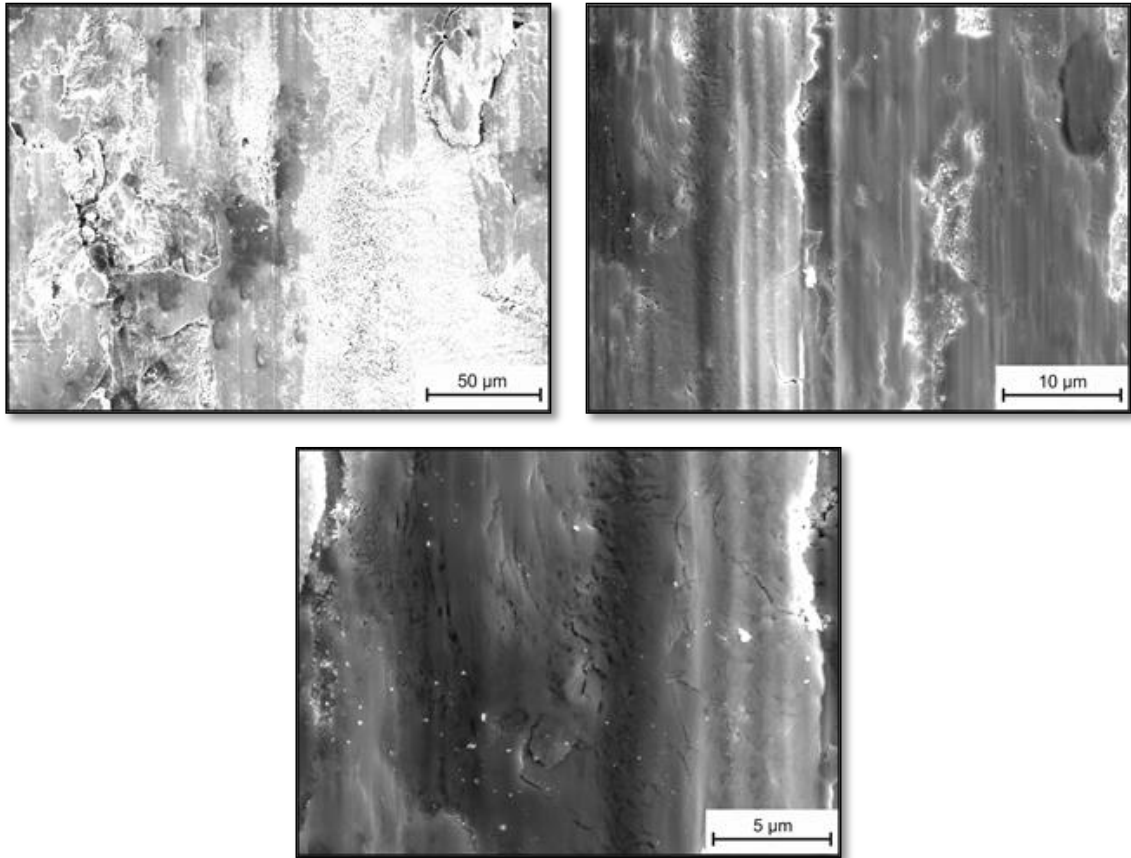


**Fig. 10:** SEM micrographs of the wear scar microstructure of HS 6-5-3, after 400°C wear test (pin: C60/ disc: HS 6-5-3)

The tribochemical wear layer of the wear test at 600°C in opposite does not show largely fractured areas. The layer appears more dense and compact. In addition wear grooves are visible which are comparable to the wear grooves appearing at room temperature (**Fig. 11**). Furthermore, the wear layer is not homogeneous. It consists of small and large particles compacted to a dense layer. Small cracks inside the layer are visible. These cracks are localized at the grooved and fractured areas. Summing up, the presented results show that the microstructural state of the wear scars of the high-speed steel depending on temperature is strongly dependent on the formation of a tribochemical wear layer during testing. The formation and influence of this wear layer is much more pronounced at elevated temperatures than at room temperature. Inside a tribological system a wear layer changes the surface characteristics of the components and thereby changes the mechanisms of friction and sliding wear. This influence is more pronounced at elevated temperatures, because thermal activated processes, like oxidation, are accelerated at elevated temperatures [16].

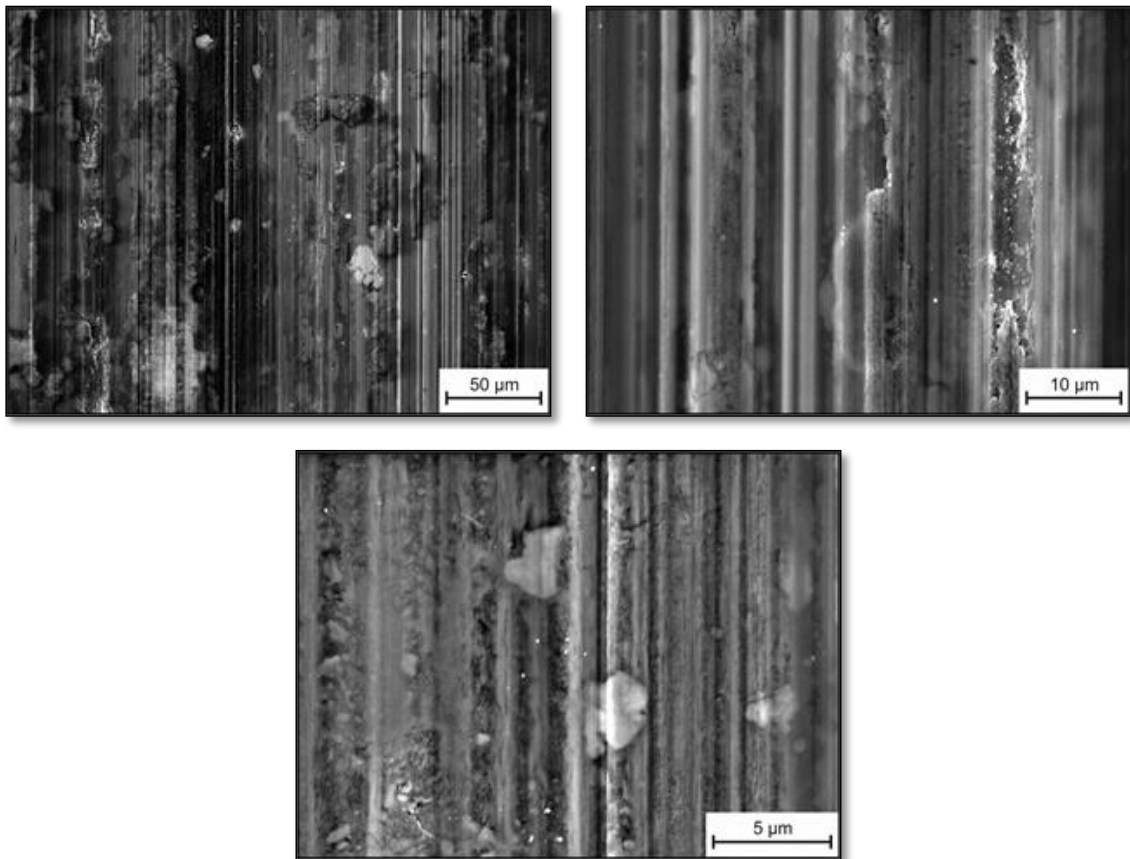


**Fig. 11:** SEM micrographs of the wear scar microstructure of HS 6-5-3, after 600°C wear test (pin: C60/ disc: HS 6-5-3)

Concluding, the high temperature wear behavior of tool materials depends on several key factors. Firstly, the microstructural constitution and the mechanical properties of the tool material at elevated temperatures are important influencing factors which decide about the performance of a material [17]. On the one hand, the material needs to bare the applied loads without fracturing. On the other hand the bulk material needs to support the formed tribochemical wear layer, to benefit from its properties. Therefore, high hardness and tensile strength at elevated temperatures improve the resistance against the impact of high temperature wear. The microstructural constitution in addition decides about the formation and stability of the formed wear layer. Hard phases can act as punctual microstructural barriers during sliding wear and are initial points of the layer formation. Thus, their distribution, size, shape, type and chemistry need to be considered. The formation of the wear layer, its stability and connection to the bulk material need to be considered as well. At elevated temperatures the characteristics of the wear layer itself are of great relevance. An increased oxidation tendency of metallic materials at elevated temperatures promotes the formation of a tribochemical layer. Therefore, the development and growth of a characteristic surface zone is much more pronounced. A formed wear layer influences sliding wear more significantly. Including a wear layer, surfaces covered by a tribochemical layer of oxides, wear particles (carbides and metal-matrix fragments) and third bodies from the ambient medium transfer the relative motion. This suppression of direct metallic contact essentially changes the characteristics of the tribological system. It is possible to decrease wear and friction and consequently improve the performance of a tool material. Nevertheless, it is also possible to damage the basic tool material by an unstable layer. A thick and brittle layer will fracture pronouncedly during application. Large areas of damaged surfaces can form and influence the process. Fractured areas act as initial points of further damages which can propagate from the surface into the bulk material leading to materials failure. Therefore, the structure and stability of the wear layer itself is a further key factor of high temperature wear. The differences of the wear layer characteristics of cemented carbides and high speed steels are depicted well by the results of



this study. Both materials respond to sliding wear at elevated temperatures with the formation of a wear layer. The structure of the wear layers nevertheless differs significantly. The temperature dependence of the layer structure varies with the basic tool material tested. At 400°C the cemented carbide material forms a tribochemical wear layer, which is well densified. Hard phases and wear products form a connected surface zone. This interaction and reciprocal support of hard phases and compacted wear products forms a self-protection of the materials and decreases wear. At a temperature of 600°C the structure of the wear layer changes significantly. The layer is more homogeneous and shows no embedded carbides. It can be assumed that the high oxidation tendency of the cemented carbide material and the C60 steel lead to a rapid growth of the tribochemical wear layer at 600°C. Overstepping a critical thickness the layer forms cracks and fractures under mechanical load. This decreases the positive influence of a high temperature wear layer. The high-speed steel moreover forms a wear layer with a dense and well compacted structure at 600°C testing temperature. In opposite to the cemented carbide material the surface zone of the high-speed steel is well densified and integrated at temperatures above 400°C. Nevertheless, the characteristics of the observed surface structures are very complex and need to consider various parameters like the oxidation tendencies and the high temperature stability of the used tool materials and its components, as well as the chemical and microstructural composition of the layer itself [18]. Therefore, further studies need to focus on the characteristics of the wear layer and its interaction with the bulk material.

### 3. Conclusions

The following key results were found within this work:

- The absolute value of the high temperature hardness of cemented carbide materials is directly dependent on the WC-carbide volume fraction, the development of the hardness with increasing temperature in opposite rather depends on the volume fraction characteristics of the matrix.
- The absolute value of high temperature hardness of high-speed steels is comparable to cemented carbide materials with larger matrix fractions. The absolute value and the temperature dependent course of the high temperature hardness of HSS are directly related to the applied heat-treatment. Therefore, they can be influenced and increased by an optimization of the heat-treatment.
- High temperature hardness and the performance of a material under high temperature sliding wear are directly correlated. A high hardness and tensile strength at elevated temperatures increase the resistance of a material against the mechanisms of wear at elevated temperatures, because of the increased support and integration of the wear affected surface zone.
- During sliding wear the cemented carbide and high-speed steel tool materials show the same temperature dependency. In the studied systems an increase in testing temperature leads to a rapid decrease of friction and wear rate.
- The reason for decreasing wear and friction is the formation of tribochemical wear layers. These layers suppress direct metallic contact and change the characteristics of the tribological system. A protection of the bulk material by the tribochemical layer occurs.
- Key issues of the topic of tribochemical wear layers are the formation and stability of these layers, their connection to and support by the bulk material, as well as the fracturing and damage of the layer-bulk-material compound.

### Acknowledgements

The authors gratefully acknowledge the financial support from the BMWI (Bundesministerium für Wirtschaft und Energie) within the project "Neue hochverschleißbeständige Werkstoffe für Umformwerkzeuge in der Stab- und Drahtherstellung". The authors also thank the company Karl Buch Walzengießerei GmbH & Co. KG for their support and cooperation.

## References

- [1] M. Nilsson, M. Olsson, *Wear*, 307 (2013), pp. 209-217
- [2] M. Pellizzari, D. Cescato, M.G. De Flora, *Wear*, 267 (2009), pp. 467-475
- [3] R. Bhattacharya, G. Jha, S. Kundu, R. Shankar, N. Gope, *Surface & Coatings Technology*, 201 (2006), pp. 526-532
- [4] W.H. Rackoff, E.L. Klaphake, Publication of Iron and Steel Society, (1990), pp. 281-306
- [5] X. Wang, K. S. Hwang, M. Koopman, Z. Fang, L. Zhang, *Int. Journal of Refractory Metals and Hard Materials*, 36 (2013), pp. 46-51
- [6] M. Lee, *Metallurgical Transactions A*, 14 A (1983), pp. 1625-1629
- [7] A. Fischer, Habilitation, Ruhr-Universität Bochum (1994)
- [8] J. Pirso, S. Letunovitš, M. Viljus, *Wear*, 257 (2004), pp. 257-268
- [9] K. Bonnya, P. De Baetsa, Y. Perezza, J. Vleugelsb, B. Lauwersc, *Wear*, 268 (2010), pp. 1504-1517
- [10] S. Balamurugan, G. Mathan, A. Dey, G. Mukherjee, M. Sahu, J.C. Pandey, *Engineering Failure Analysis*, 26 (2012), pp. 182-191
- [11] J. Wook Park, H. Choon Lee, S. Lee, *Metallurgical and Materials Transactions A*, 30A (1999), pp. 399-409
- [12] H. Qua, B. Liao, L. Liu, D. Li, J. Guoa, X. Renc, Q. Yanga, *CALPHAD: Computer Coupling of Phase Diagrams and Thermochemistry*, 36 (2012), pp. 144-150
- [13] C. Rodenburg, W.M. Rainforth, *Acta Materialia*, 55 (2007), pp. 2443-2454
- [14] H. Zhu, Q. Zhu, A. Tieu, B. Kosasih, C. Kong, *Wear*, 302 (2013), pp. 1301-1318
- [15] N.F. Garza-Montes-de-Oca, W.M. Rainforth, *Wear*, 267 (2009), pp. 441-448
- [16] Q. Zhu, H.T. Zhu, A.K. Tieu, M. Reid, L.C. Zhang, *Corrosion Science*, 52 (2010), pp. 2707-2715
- [17] A.J. Gant, M.G. Gee, *Wear*, 251 (2001), pp. 908-915
- [18] C. Rynio, Dissertation, Ruhr-Universität Bochum (2014)